THE JOURNAL OF BIOLOGICAL CHEMISTRY

Vol. 267, No. 9, Issue of March 25, pp. 6257-6262, 1992
Printed in U.S.A.

Primary Structure and Chromosomal Localization of Human and Mouse Rod Photoreceptor cGMP-gated Cation Channel*

(Received for publication, August 30, 1991)

Steven J. Pittler‡, Andrea K. Lee‡, Michael R. Altherr§, Thad A. Howard¶, Michael F. Seldin¶, Richard L. Hurwitz‖, John J. Wasmuth§, and Wolfgang Baehr‡**

From the Departments of ‡Ophthalmology, Cullen Eye Institute and ‖Pediatrics, Baylor College of Medicine, Houston, Texas 77030, the §Department of Biological Chemistry, California College of Medicine, University of California, Irvine, California 92717, and the ¶Department of Medicine and Microbiology, Duke University Medical Center, Durham, North Carolina 27710

We have determined the primary structures of the human and mouse retinal rod cGMP-gated cation channel by analysis of cDNA clones and amplified DNA. The open reading frames predicted polypeptides of 690 and 683 residues exhibiting 88% sequence similarity. Sequence comparison indicated that the rod channels consist of a variable 90-residue N-terminal region, a short highly charged segment rich in lysine and glutamate, and a 540-residue C-terminal portion that is well conserved in three mammalian species. Significant sequence similarity (59%) of the visual cGMP-gated channel to the olfactory cAMP-gated channel established the existence of a family of cyclic nucleotide-gated ion channel genes. RNA blot analysis revealed transcripts of 3.2 kilobases (kb) in human, mouse, and dog, 3.2, 4.6, and 5.2 kb in bovine, and 3.6 kb in fish. The human channel gene was mapped by polymerase chain reaction of somatic cell hybrid DNAs to chromosome 4 (p14-q13) near the centromere. The mouse channel gene locus (*Cncg*) was mapped by interspecific backcross haplotype analysis 0.9 centimorgan proximal of the *Kit* locus on chromosome 5.

Phototransduction in mammalian photoreceptors consists of a cascade of events that ultimately leads to a transient hyperpolarization of the plasma membrane (1). The change in conductance is effected by the closure of cation channels residing in the plasma membrane. In rod photoreceptors, the channel is directly and cooperatively regulated by cGMP (2), which is present at high levels in the dark keeping the channel in an open state (3). Upon activation of a cGMP phosphodiesterase, cGMP levels are lowered and the channel closes. The channel is thought to consist of a homopolymer, and in excised patches, shows a low degree of selectivity towards cations (3). The bovine channel has been purified and reconstituted into lipid vesicles as a 63-kDa polypeptide. Cloning of the bovine channel cDNA (4) revealed an open reading frame that predicts a polypeptide of 79 kDa, and its expression in *Xenopus* oocytes produced a channel activity capable of generating currents similar to the native channel (5, 6). Recently, an active 79-kDa bovine channel peptide has been purified and reconstituted into phospholipid-containing vesicles (7).

Homology cloning using bovine rod channel cDNA as a probe has allowed isolation of related olfactory cAMP-gated channel cDNAs (8, 9) establishing a cyclic nucleotide-gated channel gene family. Additionally, cGMP-gated channel activities have been characterized in kidney (10) and in cardiac pacemaker cells (11). A more distant relationship appears to exist between voltage-gated cation channels and cyclic nucleotide-gated channels, which share significant structural and sequence similarity (12). In this article, we describe the characterization of mouse and human rod cGMP-gated channel cDNAs, the deduced amino acid sequences, and the chromosome locations of the genes.

MATERIALS AND METHODS

Library Screening—A human retinal cDNA library constructed in λgt10 (provided by J. Nathans, Johns Hopkins Medical School, Baltimore, MD) and a mouse retina cDNA library in λzap (Stratagene) were screened with radiolabeled bovine rod channel (4) PCR[1] amplified fragments BCC-B and BCC-C (Fig. 1). The primers used to generate the fragments are located at positions 219–240/480–460 (BCC-B) and at 688–711/2267–2243 (BCC-C) of the bovine sequence (4). Approximately 100,000 plaque-forming units of the mouse library were screened with radiolabeled BCC-B and BCC-C. From the mouse library, 33 overlapping clones were isolated, and six clones were further characterized and completely sequenced. Screening of 500,000 plaque-forming units of the human library yielded 41 clones, three of which (HCC-1, HCC-2, and HCC-3) were further characterized.

Poly(A) mRNA Isolation, Reverse Transcription, and RNA Blotting—Poly(A) mRNA was isolated directly from mouse, bovine, and human retinas by a fast lysis oligo(dT) selection method (Fasttrack, Invitrogen). Reverse transcription of first strand cDNA was performed with 1.5 μg of RNA and 0.4 μg of mcs23 primer (13) per 25-μl reaction according to the manufacturer's protocol (Promega, Biotech). Following synthesis at 45 °C for 1 h the reaction was diluted to 250 μl with water and stored at −20 °C. For RNA blot analysis, approximately 1 μg of poly(A) was fractionated in a 0.8% agarose gel containing 2.2 M formaldehyde and transferred to a nitrocellulose membrane (14). Hybridization and washing was carried out as reported previously (15), except that 40% formamide was used.

Polymerase Chain Reaction—PCR reactions were performed in 25–400-μl volumes containing 1/25 volume of diluted cDNA, 10–20 pmol of each primer, 200 μM of each dNTP, 1.5 mM $MgCl_2$, and 0.1%

* This investigation was supported in part by an Individual National Research Service Award F32 EY06172 and a grant from the Knights Templar Eye Foundation, Inc. (to S.J.P.), National Institutes of Health Grant HG 00101 (to M.F.S.), grants from the National Eye Institute (EY06656) and the Knights Templer Eye Foundation, Inc. (to R.L.H.), a grant from the National Institute of Neurological Disease and Stroke (NS 25631) (to J.J.W.), grants from the National Eye Institute (EY08123), the National Retinitis Pigmentosa Foundation/RP Foundation, the Gund Foundation, and the Retina Research Foundation (Houston) (to W.B.). The costs of publication of this article were defrayed in part by the payment of page charges. This article must therefore be hereby marked "*advertisement*" in accordance with 18 U.S.C. Section 1734 solely to indicate this fact.

The nucleotide sequence(s) reported in this paper has been submitted to the GenBank™/EMBL Data Bank with accession number(s) M84741 and M84742.

**Recipient of a Jules and Doris Stein Research to Prevent Blindness Professorship. To whom correspondence should be sent.

[1] The abbreviations used are: PCR, polymerase chain reaction; kb, kilobase(s); RFLV, restriction fragment length variations.

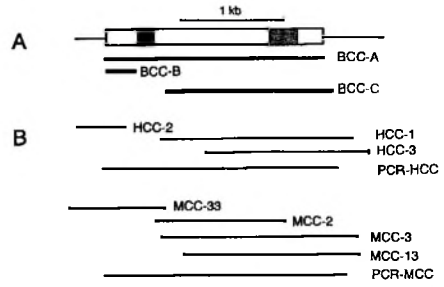

FIG. 1. **Human and mouse channel cDNA clones and PCR fragments.** *A*, schematic representation of channel cDNA. *Large rectangle*, coding sequence; *striped box*, N-terminal region encoding lysine- and glutamate-rich domain; *stippled box*, presumed cGMP-binding region. Bars marked *BCC-A*, *BCC-B*, and *BCC-C* represent PCR amplified bovine DNA used for library screening. *B*, extent of human (HCC) and mouse (MCC) cDNA clones. PCR-HCC and PCR-MCC represent PCR amplified DNA used for direct sequencing.

Triton X-100 in a Precision GTC-1 thermal cycler. Thirty-one cycles were performed as described (16).

Human Chromosome Mapping—DNA from 25 well-characterized human-hamster somatic cell hybrids was purchased from BIOS Corp. PCR was performed (16) using 50 ng of amplification primers CLF and CLR (Fig. 2), and 25 ng of DNA from each hybrid cell line in a 25-μl volume. PCR of human and hamster positive and negative control DNAs revealed the expected 295-base pair product only in the human DNA amplification. Regional mapping on chromosome 4 was done in the same manner using four additional cell hybrids, each of which retains a different segment of chromosome 4 (17, 18).

Mouse Chromosome Mapping—C3H/HeJ-*gld/gld* and *Mus spretus* (Spain) mice and [(C3H/HeJ-*gld/gld* × *Mus spretus*)F1 × C3H/HeJ-*gld/gld*] interspecific backcross mice were bred and maintained as previously described (19). *Mus spretus* was chosen as the second parent in this cross because of the relative ease of detection of informative restriction fragment length variations (RFLV) in comparison with crosses using conventional inbred laboratory strains. DNA isolated from mouse organs by standard techniques was digested with restriction endonucleases and 10-μg samples were electrophoresed in 0.9% agarose gels. DNA was transferred to Nytran membranes (Schleicher & Schuell, Inc.), hybridized at 65 °C, and washed under stringent conditions, all as previously described (20). Clones used as probes in the current study were MCC-13 (Fig. 1) and DHPR13 (QDPR) (21). Gene linkage was determined by segregation analysis (22). Gene order was determined by analyzing all haplotypes and minimizing crossover frequency between all genes that were determined to be within a linkage group. This method resulted in determination of the most likely gene order (23).

RESULTS AND DISCUSSION

Characterization of Mouse and Human Channel cDNA Clones—A composite mouse channel sequence was constructed from four overlapping clones MCC-33, MCC-2, MCC-3, and MCC-13 (Fig. 1). Since the sequence overlap between MCC-33 and MCC-3 was only 16 base pairs, oligonucleotides specific for the 5′ end of MCC-33 and the 3′ end of MCC-3 were used to amplify a full-length channel cDNA (PCR-MCC, Fig. 1). By means of unique restriction sites introduced at the 5′ ends of the primers, the amplified material was cloned into a plasmid vector and sequenced. The sequence obtained is in complete agreement with the composite sequence shown in Fig. 2 indicating that the MCC clones depicted in Fig. 1 derive from one mRNA species. Sequence analysis of human clones HCC-1, HCC-2, and HCC-3 (Fig. 1) showed that the majority of the coding sequence could be determined, with the exception of an A-rich segment near the 5′ end. To complete the sequence of the human channel cDNA, oligonucleotide primers were designed from the sequence determined in the 5′- and 3′-untranslated regions of clones HCC-2 and HCC-3, respectively, and cDNA was amplified and directly sequenced without cloning. The sequences of the overlapping clones and the PCR fragment (PCR-HCC, Fig. 1) were in complete agreement yielding the sequence shown in Fig. 2.

cDNA Sequence of the Mouse and Human Rod Channel—The cDNA sequences shown in Fig. 2 contain open reading frames of 2076 and 2082 nucleotides for the mouse and human channel, respectively. Translation initiation of the mouse channel is assigned to the first ATG (position 1 in Fig. 2) 24 nucleotides downstream of an in-frame stop codon, and of human to an ATG 12 nucleotides downstream. Both initiators are preceded by a ribosome binding consensus sequence (24). Curiously, the human cDNA sequence predicts an extended N terminus consisting of 4 amino acids, MKLS, which are not present in mouse or bovine (Fig. 4). The overall sequence similarity between the mouse and human channel coding sequences is 85%, the highest sequence variation is found near the N- and C-termini. The 3′-untranslated region shown in Fig. 2 does not contain polyadenylation signals indicating that the 3′ regions are incomplete. PCR analysis of retina cDNA with a channel specific primer and an anchoring primer specific for the poly(A) tail (13) indicates that the distance between the last nucleotide shown in Fig. 2 and the poly(A) tail is approximately 150 nucleotides (results not shown).

RNA Blot Analysis—Using the near full-length PCR product PCR-HCC (Fig. 1) as a probe in Northern blots, the predominant transcript detected in human, bovine, mouse, and dog retinas is a 3.2-kb species (Fig. 3). In bovine, additional transcripts of 4.6 and 5.2 kb are also observed. Since the larger transcripts are not detected in human and mouse, they are unlikely to represent related products of another gene, but are more likely due to alternate poly(A) site usage as found for opsin mRNAs in several species (13). The high degree of conservation of the channel sequence is exemplified by the signal observed in the lane containing red fish RNA (Fig. 3; *lane 1*). Northern analysis of various rat tissues demonstrated hybridization signals only in kidney and heart (25), consistent with the presence of homologous channel genes in these tissues.

The N-terminal Domain of the Rod Channel—The cDNA sequences predict 690 and 683 amino acid polypeptides for the human and mouse rod channel both of which contain five potential *N*-linked glycosylation sites. Two of these sites are present in the olfactory and visual channels at approximately identical positions (Fig. 4). The bovine rod channel was previously shown to contain at least one carbohydrate chain that could be removed by treatment with glycopeptidase F (26). The functional significance of carbohydrate side chains in mammalian channels, all of which appear to be glycosylated, is unknown.

The sequence variation between rod channels (bovine, mouse, human) is greatest in the N-terminal region; an alignment of the three sequences is only possible when several gaps are introduced (Fig. 4). An unusual structural feature of the rod channel is an extremely hydrophilic 57–58 residue N-terminal domain predicted to consist of 29 lysines (no arginines) and 19 glutamic/aspartic acid residues (Fig. 4). Most channel purifications yield a protein of 63 kDa indicating that cleavage may occur near or in this domain removing an approximately 16-kDa moiety. This cleaved domain may also contain the binding site for the Ca^{2+} channel blocker L-*cis*-diltiazem, since the purified 63-kDa channel is insensitive (4), but the 79-kDa channel is sensitive to the inhibitor (7). Except for an insertion of 1 additional glutamic acid in bovine and mouse, and the replacement of 2 glutamic acid residues for 2 histidines in human, the charged domain is well conserved

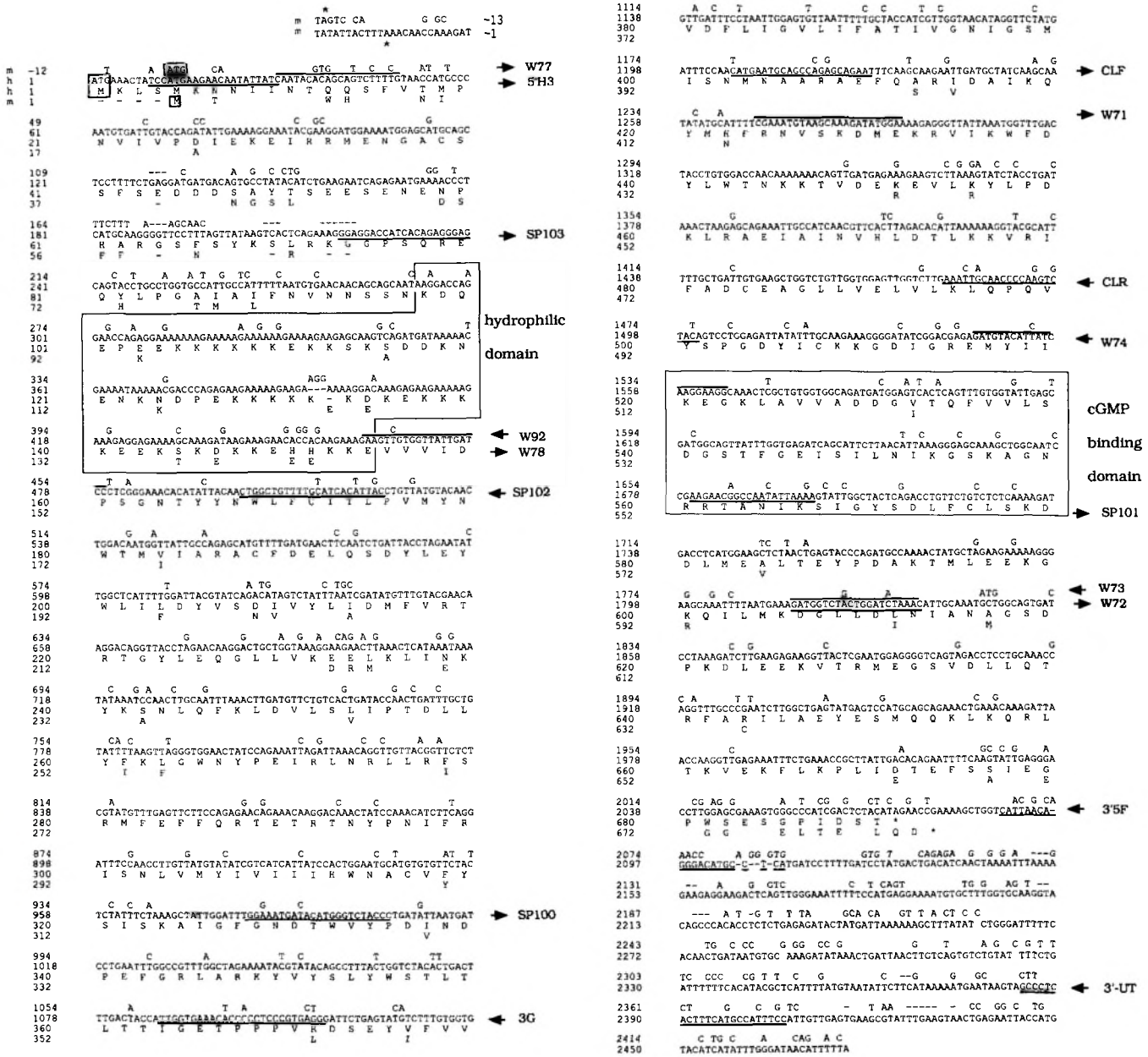

FIG. 2. **Complete cDNA sequence of human and mouse cGMP-gated channel.** The human cDNA and amino acid sequences (*h*) are shown as continuous sequences, and nucleotide and amino acid differences in the respective mouse sequences are indicated above and below the human sequence. Nucleotide numbering starts with A of the presumed translation initiator codon ATG (*boxed*), amino acid numbering with the initiator methionine (*M*, *boxed*). *Asterisks* delimit the open reading frames. *Hyphens* in the mouse and human sequences indicate gaps. Primer sequences used for sequence analysis or amplification are *underlined*, and their orientations are indicated on the right margin by an *arrow*. The *boxed* areas denote an A-rich region (hydrophilic domain) and the presumed cGMP-binding domain.

between the three species. The hydrophilicity within this region is less pronounced (20 charged residues) in corresponding olfactory channel domains which are also 6 residues shorter. Interestingly, the only uncharged amino acid that is conserved between olfactory and visual channel charged domains is a central proline (Fig. 4).

Potential Transmembrane Domains—Hydrophobicity plots indicate at least six hydrophobic amino acid sequences of 20 residues or more, termed H1–H6 (4), perhaps representing transmembrane domains (Fig. 4). Since both N and C termini are presumed to be intracellular, an even number of transmembrane domains (2, 4, 6, or more) is required. In terms of amino acid conservation, H6 is perfectly conserved between the three species, and H1 has only one minor substitution. H2–5 have several, mostly conservative substitutions not perturbing the hydrophobicity of the domains. H1, H2, H5, and H6 have 1–4 mostly negative charges all of which are perfectly conserved in human, mouse, and bovine. At least some of these charges may be involved in amphipathic helical structures forming part of the actual channel pore (28). Surprisingly, a voltage sensor motif RLN-RLL-RFS-RMF identified in voltage-gated cation channels and thought to be part of the membrane structure, is also present in rod and olfactory channels. Since the gating of rod channels shows only weak

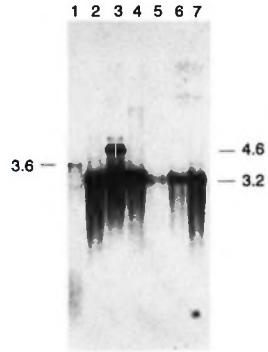

FIG. 3. **RNA blot analysis of the cGMP-gated channel in various species.** Approximately 1 μg of poly(A) mRNA was loaded per lane. *Lane 1*, redfish; *lane 2*, human; *lane 3*, bovine; *lane 4*, normal mouse; *lane 5*, *rd* mouse; *lane 6*, dog affected with progressive retinal degeneration (38); *lane 7*, normal (heterozygous) dog. Radiolabeled PCR-HCC fragment (Fig. 1) was used as a probe. Sizes of major RNA species are shown to the left and right as determined form a standard curve of a RNA ladder (BRL, Bethesda).

voltage dependence (4), its importance may be in preserving the protein core structure (12).

Cyclic Nucleotide-binding Domain—Homology to bovine lung cGMP-dependent protein kinase predicts 1 cGMP binding site/channel polypeptide (4). Since cGMP-binding studies indicate a Hill coefficient of 3–4 (6, 7), an oligomeric structure is proposed for the functional channel. The cGMP-binding domain (position 500–587 of the human sequence in Fig. 4) is the best conserved domain between the three species, containing only one conservative substitution (valine *versus* isoleucine at position 532). Two of the 4 cysteines conserved in olfactory and visual channel sequences are located at the border of this domain suggesting their importance for proper folding and function of the polypeptide.

Chromosome Mapping of the Human Channel Gene—Molecular defects in the rod channel could lead to malfunction of the phototransduction cascade and inability to generate a nerve impulse causing blindness. A defective rod channel gene thus is a possible candidate gene for human retinitis pigmentosa or related retinal disorders. In order to identify the chromosome location of the human gene (locus designation CNCG), we performed PCR analysis on DNAs from 25 human-hamster somatic cell hybrids. The primers CLF and CLR (Fig. 2) amplify an intronless 295-base pair human-specific fragment (not shown). As noted in Table I only hybrids 803 and 1006 (and the human control DNA) yielded the expected PCR product consistent with the human cGMP-gated channel gene residing on chromosome 4. To narrow down the location of the gene to a specific region of chromosome 4, we performed PCR on DNA isolated from four radiation hybrids that contain only partial segments of chromosome 4 (Fig. 5). The absence of hybridization to DNA from hybrids 693 and 848 and the positive signals obtained with hybrids 842 and 892 demonstrate that the gene is contained within the region p14-q13.

Chromosome Mapping of the Mouse Channel Gene—In order to determine the chromosomal location of the mouse cGMP-gated channel gene (locus designation *Cncg*), we utilized a panel of DNA samples from an interspecific cross that has been characterized for over 375 genetic markers throughout the genome. The genetic markers included in this map span between 50 and 80 centimorgans on each mouse autosome and the X chromosome (for examples, see Refs. 19 and 29). DNA from the two parental mice [C3H/HeJ-*gld*/*gld* and (C3H/HeJ-*gld*/*gld* × *Mus spretus*)F1] were digested with various restriction endonucleases and hybridized with radiolabeled *Cncg* cDNA (MCC-13, Fig. 1) to determine an RFLV to allow haplotype analyses. An informative RFLV was detected with *Bgl*II restricted DNAs (Fig. 6*B*). Each of 114 *Bgl*II-restricted DNAs from the [C3H/HeJ-*gld*/*gld* × (C3H/HeJ-

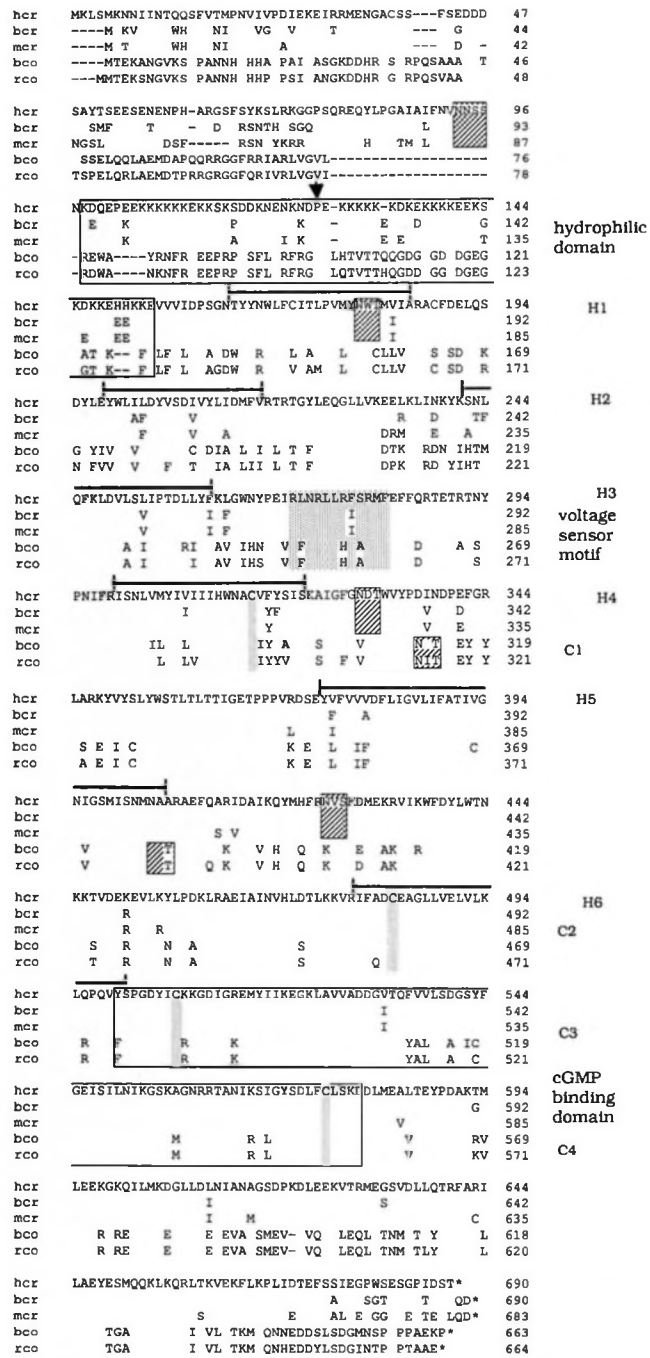

FIG. 4. **Sequence comparison of cyclic nucleotide-gated channels.** An alignment of the amino acid sequences of the human (*hcr*), bovine (*bcr*) (4), and mouse (*mcr*) cGMP-gated channels, and bovine (*bco*) and rat (*rco*) olfactory cAMP-gated channels (8, 9) is shown. The lysine/glutamate-rich region near the N termini ("hydrophilic domain") and the cGMP-binding domain near the C termini are depicted within *large boxes*. The *stippled box* indicates the domain with resemblance to the voltage sensor motif (9) in voltage-gated channels. *Striped boxes* identify the positions of conserved potential *N*-linked glycosylation sites. Putative transmembrane domains (H1–H6) are marked by a *black cross-bar*, and the four invariant cysteines (C1–C4) are *shaded*. An invariant proline in the hydrophilic domain is marked by a *vertical arrow*.

TABLE I

Segregation of cGMP-gated channel gene in human-hamster somatic cell hybrids

		Human Chromosomes[b]																						
Hybrids[a]	CNCG	1	2	3	4	5	6	7	8	9	10	11	12	13	14	15	16	17	18	19	20	21	22	X	Y
1) 324	−	−	−	−	−	−	−	−	−	−	−	−	−	−	−	−	−	−	+	−	−	−	−	−	−
2) 423	−	−	−	+	−	−	−	−	−	−	−	−	−	−	−	−	−	−	−	−	−	−	−	−	−
3) 734	−	−	−	−	−	+	−	−	−	+	−	−	−	−	−	−	−	−	+	−	−	−	−	−	−
4) 750	−	−	−	−	−	D	−	−	−	−	−	−	−	+	+	+	−	−	−	+	−	−	−	−	−
5) 803	+	−	−	−	+	+	−	−	+	−	−	15	−	−	−	−	−	−	−	−	−	−	+	+	−
6) 860	−	−	−	15	−	+	+	−	−	−	15	−	−	−	−	−	−	−	−	45	−	+	−	−	−
7) 867	−	−	−	−	−	+	−	−	−	−	−	−	−	+	+	−	−	−	+	+	−	−	−	−	−
8) 940	−	−	−	−	−	+	−	−	−	−	−	−	−	−	−	−	−	−	−	−	+	−	−	−	−
9) 212	−	−	−	−	−	Dq	−	−	−	−	−	−	−	−	−	−	−	−	−	−	−	−	−	−	+
10) 507	−	−	−	+	−	+	−	−	−	−	−	−	+	−	+	−	−	−	−	−	40	−	25	−	+
11) 683	−	−	−	−	−	+	−	−	−	−	−	11	45	−	+	−	−	−	−	+	−	+	+	−	−
12) 756	−	−	−	−	−	D	+	+	−	−	−	−	+	+	45	−	−	−	−	+	+	+	−	−	+
13) 811	−	−	−	−	−	−	−	−	+	−	−	−	−	−	−	−	−	+	+	−	−	−	−	−	−
14) 983	−	−	−	−	−	+	−	−	−	−	+	−	−	−	−	−	−	−	−	−	−	−	−	−	−
15) 862	−	−	−	−	−	+	−	−	−	+	−	−	−	−	−	−	−	−	−	−	−	−	−	−	−
16) 909	−	−	−	−	−	D	+	−	+	−	−	−	−	−	+	−	−	−	−	−	−	−	−	+	−
17) 937	−	−	−	−	−	+	−	−	−	−	−	−	−	−	+	+	−	+	−	−	−	+	−	−	−
18) 854	−	−	+	−	−	+	−	−	−	−	−	−	−	−	−	−	−	−	−	−	−	−	−	−	−
19) 904	−	−	−	−	−	D	+	−	−	−	−	−	+	−	−	−	5	−	−	−	−	+	−	−	+
20) 967	−	−	−	−	−	+	−	−	+	−	−	−	−	−	−	−	+	−	−	−	−	−	−	−	−
21) 968	−	−	−	−	−	+	−	−	−	+	−	−	−	+	−	−	−	−	−	−	−	−	−	−	−
22) 1006	+	−	−	−	55	+	−	+	+	−	−	−	−	+	−	+	−	−	−	+	−	+	−	−	−
23) 1049	−	−	−	−	−	+	−	−	−	−	−	+	−	−	−	−	−	−	−	−	−	−	−	−	−
24) 1079	−	−	−	+	−	+	−	−	−	−	45	−	−	−	−	10	+	−	−	−	−	−	−	−	−
25) 1099	−	−	−	−	−	D	−	−	−	−	−	−	−	+	−	−	−	−	−	+	−	+	+	−	60
[c]# Disc.		2	3	5	0	14	6	2	3	5	4	2	6	6	9	3	4	4	6	7	5	7	3	2	6

[a] D, deleted at 5p15.1 − 5p15.2; Dq, multiple deletions in 5q.
[b] Numbers are the percentage of the cell population containing the noted chromosome; "+" = >75%.
[c] Presence of chromosome counted only if greater than 30%.

FIG. 5. **Regional localization of the human cGMP-gated channel gene.** Shown to the right of the idiogram of human chromosome 4 are *vertical lines* representing the portion of the chromosome contained in each of four human-hamster somatic cell hybrids. The number of each hybrid cell line and the presence (+) or absence (−) of the expected PCR product is indicated below. The PCR results are consistent with regional localization of 4p14–4q13 marked by the *bracket* to the left of the diagram.

gld/gld × *Mus spretus*)F1] interspecific backcross mice displayed either the homozygous (CC) or heterozygous (SC) F1 pattern when hybridized with the MCC-13 *Cncg* probe (data not shown).

Comparison of the haplotype distribution of the *Pdc* RFLV indicated that in 113 of 114 meiotic events examined, the *Cncg* locus co-segregated with *Kit* (Fig. 6*A*), a locus previously mapped to mouse chromosome 5 (30). This result indicated that *Cncg* was linked with *Kit* (the probability of linkage is >0.99; upper 95% confidence limit by binomial distribution = 4.6 centimorgans). The haplotype distribution among other genes localized to mouse chromosome 5 is shown in Fig. 6*A*. The best gene order (23) ± the standard deviation (22) indicated that the mouse *Cncg* locus was located 9.6 ± 2.8 centimorgans distal to *Qdpr* and 0.9 ± 0.9 centimorgan proximal of *Kit*. The position of *Cncg* on mouse chromosome 5 and the location of the human homologue on the short arm of chromosome 4 provided evidence that this gene is another member of a linkage group conserved between these chromosomal segments (31, 32).

Functional channel polypeptides are critically important for transport of cations and anions through the plasma membrane. For example, a defect in a cAMP-regulated chloride channel gene, located on human chromosome 7, is thought to cause cystic fibrosis (330. The shaker locus of *Drosophila* encodes a potassium channel in which defects produce neurological disturbances (34). Currently, the rod cGMP-gated channel gene is not known to be linked to any hereditary retinal dystrophy. Since high levels of channel mRNA of the same size (3.2 kb) are also found in kidney even at very high stringency of hybridization and wash conditions (25), it ap-

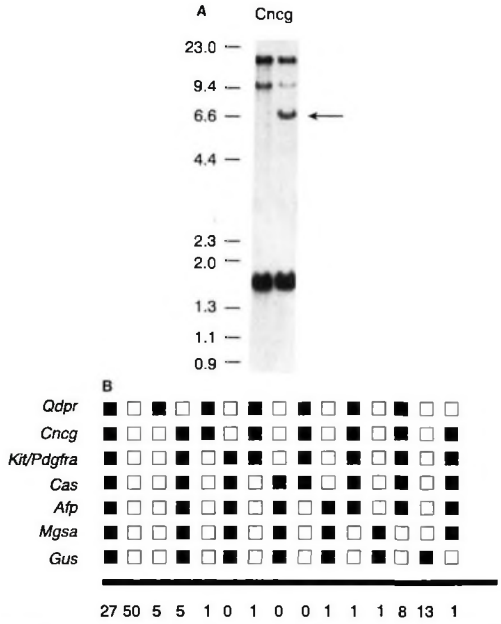

FIG. 6. **Regional localization of the mouse cGMP-gated channel gene.** *A*, Southern blot identification of a *Cncg* RFLV. The informative *Bgl*II restriction digest is shown with the molecular size standards (in kb) indicated to the left of the panel. The *arrow* signifies a band present in DNA from (C3H/HeJ-*gld*/*gld* × *Mus spretus*)F1 (SC) mice that are not present in DNA from C3H/HeJ-*gld*/*gld* mice (CC). *B*, segregation of *Cncg* among mouse chromosome 5 loci in [(C3H/HeJ-*gld*/*gld* × *Mus spretus*)F1 × C3H/HeJ-*gld*/*gld*] interspecific backcross mice. *Closed boxes* represent the homozygous C3H pattern and *open boxes* the F1 pattern. The segregation of *Kit*, *Pdgfra*, *Cas*, *Afp*, *Mgsa*, and *Gus* have been previously examined (31, 32). *Qdpr* RFLVs were determined using *Eco*RI restricted DNAs (C3H: 9.5- and 6.8-kb bands; *Mus spretus*: 8.2-kb band).

pears that both channel mRNAs may be transcribed from the same gene. Moreover, only one gene locus has been identified by hybridization (Fig. 6) with mouse channel cDNA probes. It is unlikely, however, that the cGMP-inhibited channel characterized by patch clamping in kidney (10) is derived from the same gene as the cGMP-gated rod channel, since the two channels have different functional properties. A search of the OMIM (Online Mendelian Inheritance in Man, V. McKusick, Johns Hopkins Medical School, Baltimore) data base for disorders with pleiotropic effects in which a defective channel may be causative identified an hereditary renal-retinal dysplasia. This rare disorder presents with the combined pathologies of familial juvenile nephronophthisis and Leber's congenital amaurosis, a form of retinitis pigmentosa (35, 36). The findings of abnormal electroretinograms (37) and kidney dysfunction are consistent with a possible channel defect. Another more common disorder exhibiting pleiotropic effects is the Bardet-Biedl syndrome which is often accompanied by retinal degeneration, nephropathy, and mental retardation. Unfortunately, while both of these disorders display an autosomal recessive mode of inheritance, neither has been assigned to a specific chromosome. Linkage analysis is currently being performed to rule out a channel gene defect in patients with these disorders.

Acknowledgments—We thank M. Champagne and V. Holcombe for technical assistance, U. B. Kaupp for providing the sequence of the bovine channel prior to publication, G. I. Liou for fish and human retinal RNA, J. F. McGinnis for mouse 9–11-day-old *rd* mRNA, and R. H. Lee and R. N. Lolley for Irish setter dog retinas.

REFERENCES

1. Stryer, L. (1988) *Cold Spring Harbor Symp. Quant. Biol.* **53,** 283–294
2. Fesenko, E. E., Kolesnikov, S. S., and Lyubarski, A. L. (1985) *Nature* **313,** 310–313
3. Yau, K.-W., and Baylor, D. A. (1989) *Annu. Rev. Neurosci.* **12,** 289–327
4. Kaupp, U. B., Niidome, T., Tanabe, T., Terada, S., Boenigk, W., Stuehmer, W., Cook, N. J., Kangawa, K., Matsuo, H., Hirose, T., Miyata, T., and Numa, S. (1989) *Nature* **342,** 762–766
5. Cook, N. J., Zeilinger, C., Koch, K. W., and Kaupp, U. B. (1986) *J. Biol. Chem.* **261,** 17033–17039
6. Cook, N. J., Hanke, W., and Kaupp, U. B. (1987) *Proc. Natl. Acad. Sci. U. S. A.* **84,** 585–589
7. Hurwitz, R., and Holcombe, V. (1991) *J. Biol. Chem.* **266,** 7975–7977
8. Dhallan, R. S., Yau, K.-W., Schrader, K. A., and Reed, R. R. (1990) *Nature* **347,** 184–187
9. Ludwig, J., Margalit, T., Eismann, E., Lancet, D., and Kaupp, U. B. (1990) *FEBS Lett.* **270,** 24–29
10. Light, D. B., Corbin, J. D., and Stanton, B. A. (1990) *Nature* **344,** 336–339
11. DiFrancesco, D., and Tortora, P. (1991) *Nature* **351,** 145–147
12. Jan, L. Y., and Jan, Y. N. (1990) *Nature* **345,** 672
13. Al-Ubaidi, M. R., Pittler, S. J., Champagne, M. S., Triantafyllos, J. T., McGinnis, J. F., and Baehr, W. (1990) *J. Biol. Chem.* **265,** 20563–20569
14. Thomas, P. (1980) *Proc. Natl. Acad. Sci. U. S. A.* **77,** 5201–5205
15. Pittler, S. J., Baehr, W., Wasmuth, J. J., McConnell, D. G., Champagne, M. S., VanTuinen, P., Ledbetter, D., and Davis, R. L. (1990) *Genomics* **6,** 272–283
16. Pittler, S. J., and Baehr, W. (1991) *Proc. Natl. Acad. Sci. U. S. A.* **88,** 8322–8326
17. Tabas, J. A., Zasloff, M., Wasmuth, J. J., Emanuel, B. S., Altherr, M. R., McPherson, J. D., Wozney, J. M., and Kaplan, F. S. (1991) *Genomics* **9,** 283–289
18. Smith, B., Skarecky, D., Bengtsson, U., Magenis, R. E., Caprenter, N., and Wasmuth, J. J. (1991) *Am. J. Hum. Genet.* **42,** 335–344
19. Seldin, M. F., Howard, T. A., and D'Eustachio, P. (1989) *Genomics* **5,** 24–28
20. Ausubel, F. M., Brent, R., Kingston, R. E., Moore, D. D., Smith, J. A., Seidman, J. G., and Struhl, K. (1987) *Current Protocols in Molecular Biology,* Wiley Interscience, New York
21. Lockyer, J., Cook, R. G., Milstien, S., Kaufman, S., Woo, S. L. C., and Ledley, F. D. (1987) *Proc. Natl. Acad. Sci. U. S. A.* **84,** 3329–3333
22. Green, E. L. (1981) *Genetics and Probability in Animal Breeding Experiments* (Green, E., ed) pp. 77–113, McMillan, New York
23. Bishop, D. T. (1085) *Genet. Epidemiol.* **2,** 349–361
24. Kozak, M. (1987) *Nucleic Acids Res.* **15,** 8125–8132
25. Ahmad, I., Redmond, L. J., and Barnstable, C. J. (1990) *Biochem. Biophys. Res. Commun.* **173,** 463–470
26. Wohlfart, P., Müller, H., and Cook, N. J. (1989) *J. Biol. Chem.* **264,** 20934–20939
27. Hejne, G. V. (1986) *Nucleic Acids Res.* **14,** 4683–4690
28. Jennings, M. L. (1989) *Annu. Rev. Biochem.* **58,** 999–1027
29. Saunders, A. M., and Seldin, M. F. (1990) *Genomics* **8,** 525–535
30. Geissler, E. N., Ryan, M. A., and Housman, D. E. (1988) *Cell* **55,** 185–192
31. Seldin, M. F., Martinez, L., Howard, T. A., Naylor, S. L., and Sakaguchi, A. Y. (1990) *Cytogen. Cell Genet.* **54,** 68–70
32. Smith, E. A., Seldin, M. F., Martinez, L., Watson, M. L., Choudhury, G. G., Lalley, P. A., Pierce, J., Aaronson, S., Barker, J., Naylor, S. L., and Sakaguchi, A. Y. (1991) *Proc. Natl. Acad. Sci. U. S. A.* **88,** 4811–4815
33. Higgins, C. F., and Hyde, S. C. (1991) *Nature* **352,** 194–195
34. Timpe, L. C., and Jan, L. Y. (1987) *J. Neurosci.* **7,** 1307–1317
35. Senior, B., Friedmann, A. I., and Braudo, J. L. (1961) *Am. J. Ophthalmol.* **52,** 625–633
36. Godel, V., Iaina, A., Nemet, P., and Lazar, M. (1979) *Clin. Genet.* **16,** 277–281
37. Hogewind, B. L., Veltkamp, J. J., Polak, B. C. P., and van Es, L. A. (1977) *Acta Med. Scand.* **202,** 323–326
38. Aguirre, G., Farber, D. B., Lolley, R. N., Fletcher, R. T., and Chader, G. J. (1978) *Science* **201,** 1133–1134